

Porous metal organic framework nanoparticles to address the challenges related to busulfan encapsulation

Busulfan is an alkylating agent widely used in chemotherapy, but with severe side effects. Many attempts have been made to entrap busulfan in nanocarriers to avoid liver accumulation and to protect it against rapid degradation in aqueous media. However, poor loadings (≤ 5 wt%) and fast release were generally obtained due to the low affinity of busulfan towards the nanocarriers. Moreover, drug crystallization often occurred during nanoparticle preparation. To circumvent these drawbacks, metal organic framework (MOF) nanoparticles, based on crystalline porous iron (III) carboxylates, have shown an unprecedented loading (up to 25 wt%) of busulfan. This was attributed to the high porosity of nanoMOFs as well as to their hydrophilic–hydrophobic internal microenvironment well adapted to the amphiphilic character of busulfan. NanoMOFs formulations have kept busulfan in molecular form, preventing its crystallization and degradation. Indeed, busulfan was released intact, as proved by the maintenance of its pharmacological activity.

KEYWORDS: busulfan • cytotoxicity • drug crystallization • drug loading • drug release • iron (III) carboxylate • nanoparticle • NMR • porous MOF

Busulfan (1,4-butanediol-dimethylsulfonate) is a bifunctional alkylating agent [1], widely used in combination high-dose chemotherapy regimens followed by allogeneic or autologous hematopoietic stem-cell transplantation (HSCT) for the treatment of hematological malignancies [2] and nonmalignant disorders such as immunodeficiency [3]. For a long time, busulfan has only been available orally [4,5], but a wide intra-patient and inter-patient bioavailability variability in both adult and children has been reported [6]. Moreover, important side effects have been described during these treatments. Hepatic veno-occlusive disease (HVOD) is the most severe and frequent high risk injury [7,8]. Liver toxicity has been correlated with a high systemic exposure to busulfan, expressed as the area under the plasma concentration–time curve [9,10].

An intravenous busulfan formulation has been shown to be an interesting method to improve HSCT [11]. However, this approach was hindered by the low solubility of busulfan and its poor stability in aqueous medium [12]. More recent developments were achieved by dissolving busulfan in water miscible solvents such as *N,N*-dimethylacetamide (DMA) [13] or dimethylsulfoxide (DMSO) containing low molecular weight polyethylene glycol (PEG) [14]. These formulations were able to reduce the inter-patients and intra-patient bioavailability variations observed after oral administration and to decrease the incidence of HVOD during HSCT [15,16].

However, both DMA and DMSO have their own well documented toxicity and therefore, to avoid the massive use of these organic solvents, injectable colloidal carriers, such as liposomes [17], Spartaject™, a micro-suspension, [18] as well as biodegradable polymer nanoparticles (NPs) [19] have been proposed. However, the main drawback of all existing intravenous busulfan nanocarriers is their low payloads, usually lower than 1% (w/w). For example, busulfan loading in poly(lactic acid) NPs was only 1% (w/w) [19] due to a massive drug leakage from the NPs during their preparation. In more recent studies, some of us have established the ability of biodegradable poly(isobutyl cyanoacrylate) (PIBCA) NPs to encapsulate larger amounts of busulfan than other polymers [20]. Moreover, these busulfan-loaded PIBCA NPs with 6 wt% loading were successfully coated with a PEG shell [21], could be stored after freeze drying [22], but showed a fast release.

Therefore, the entrapment of busulfan in nanocarriers with loadings higher than 6 wt% is a clearly identified challenge [23]. The main problems related to the poor loadings and uncontrolled drug release were recently identified as: the high tendency of busulfan to crystallize in aqueous media and its low affinity for the biodegradable polymer matrices [23]. Indeed, for safe administration, the NP suspensions should not contain free busulfan crystals, which is another important challenge [24].

T Chalati¹, P Horcajada^{1,2},
P Couvreur¹, C Serre²,
M Ben Yahia³, G Maurin³
& R Gref^{†1}

¹ Faculté de Pharmacie (UMR CNRS 8612), Université Paris-Sud, 92296 Châtenay-Malabry Cedex, France.

² Institut Lavoisier (UMR CNRS 8180), Université de Versailles, 78035 Versailles Cedex, France.

³ Institut Charles Gerhardt Montpellier (UMR CNRS 5253), Université Montpellier 2, 34095 Montpellier cedex 05, France.

[†] Author for correspondence: ruxandra.gref@u-psud.fr horcajada@chimie.uvsq.fr

future
medicine part of fsg

In this context, we propose a completely new approach by using hybrid crystalline porous solids (or metal-organic frameworks [MOFs]). MOFs or coordination polymers are built up from the assembly, exclusively by strong ionic-covalent bonds, of inorganic sub-units and easily tunable organic linkers (carboxylates, phosphonates, imidazolates, etc.), leading to crystalline frameworks with sometimes very high and regular porosities [25]. Moreover, the high structural flexibility of some porous MOFs [26] enables the adaptation of their porosity to the shape of the hosted molecule. Recently, nanoMOFs based on NPs of non toxic porous iron(III) carboxylates, were shown to exhibit important drug loadings and progressive release as well as interesting imaging properties [27]. These nanodevices with their internal simultaneously hydrophilic and hydrophobic microenvironment make them ideal candidates for a new valuable solution concerning busulfan administration. Indeed, to address the above mentioned challenges, our aim was to investigate busulfan entrapment using four different rigid or flexible porous iron(III) MOF NPs:

- The flexible microporous MIL-53, based on a terephthalate linker and trans chains of iron octahedra sharing OH groups, creating a three-dimensional framework with a monodimensional channel system (~ 8.5 Å), [28];
- The rigid mesoporous cubic zeotypic MIL-100, built from trimers of iron(III) octahedra and trimesate anions, showing two types of mesoporous spherical cages; while larger ones (~ 29 Å) are accessible through hexagonal (~ 8.6 Å) and pentagonal ($\sim 4.8 \times 5.8$ Å) windows, smaller cages (~ 25 Å) are accessible exclusively through pentagonal windows [29];
- Flexible iron fumarate MIL-88A (~ 6 Å)
- Flexible iron muconate MIL-89 (~ 11 Å) [26,30–33].

MIL-88A and MIL-89 solids, which are based on trimers of iron(III) octahedral and dicarboxylates linkers, exhibit a three-dimensional structure with an interconnected pores and cages system, able to modulate the pore size according to the host molecule.

After synthesis and characterization of the porous nanoMOFs, we describe here a simple one-step method to efficiently entrap busulfan. In addition, a NMR procedure has been developed to assess busulfan release. Complementary molecular simulations based on periodic density functional theory calculations are also presented

to shed some light on the preferential arrangement of busulfan in the flexible MIL-53 solid and its resulting interaction energy. Finally, the *in vitro* cytotoxicity of the drug-loaded NPs is evaluated.

Materials & methods

■ Synthesis

Nanoparticles

Different synthesis methods were set up to obtain NPs of rigid or flexible MOFs [27,33].

MIL-88A: MIL-88A was obtained by microwave assisted hydrothermal synthesis from 10 ml of an aqueous solution of $\text{FeCl}_3 \cdot 6\text{H}_2\text{O}$ (10 mM) and fumaric acid (10 mM) heated at 80°C for 2 min under continuous stirring. (600 Watts; Mars 5, CEM: Power maximum output $1600 \text{ W} \pm 15\%$; Frequency at full power 2450 MHz; USA) [27,33].

MIL-89: The synthesis was performed by solvothermal route [27] from a solution of iron (III) acetate (1 mmol; obtained as previously reported by Dziobkowski [34] and trans,trans-muconic acid (1 mmol; 97%, Fluka) in 5 ml of methanol (99.9%, Aldrich) with 0.25 ml of sodium hydroxide 2M (98%, Alfa Aesar) placed into a Teflon-lined steel autoclave at 100°C for 6 h.

MIL-53: The synthesis was performed from a solution of $\text{FeCl}_3 \cdot 6\text{H}_2\text{O}$ (1 mmol) and terephthalic acid (1 mmol; 1,4-BDC; 98%, Aldrich) in 5 ml DMF by solvothermal route at 150°C for 2 h. [27]

MIL-100: NPs were obtained from a solution of Fe metal (8 mmol; 99%, Waco), 1,3,5-benzenetricarboxylic acid (5.3 mmol; 1,3,5, BTC; 95%, Aldrich), HF (4 mmol; HF, 48% in water, Aldrich) in 40 ml of water using an autoclave at 200°C for 30 min under microwave irradiation at 600 W, with a heating ramp of 2 min [27].

The obtained NPs were recovered by centrifugation at 5600 g for 10 min. To remove the solvent and the residual non reacted organic acids, 200 mg of NPs were suspended in 100 ml of deionized water, in the case of MIL-88A, or in 100 ml of absolute ethanol (99%, Aldrich), in the case of MIL-89, MIL-53 and MIL-100 overnight. The activated NPs were then recovered by centrifugation at 5600 g for 10 min and dried at room temperature.

The morphology of the purified nanosolids was analyzed by transmission electron microscopy (TEM; Darwin ; 208 Philips; 60–80–100 KV; Camera AMT) and scanning electron microscopy (SEM ; LEO 1530, LEO Electron Microscopy Inc, Thornwood, USA, 3 KV). The size distribution of the MOF NPs was

estimated by dynamic light scattering (DLS) using a Malvern® Nano-ZS (Zetasizer Nano series, UK).

In addition, x-ray powder diffraction (XRPD) patterns were collected in a conventional high resolution (θ - 2θ) D5000 Bruker diffractometer (λ Cu K α , K α_2) from 3 to 20° (2 θ) using a step size of 0.02° and 4 s per step in a continuous mode.

Microparticles

Additionally, MIL-100 microparticles (micro-crystals) were synthesized as previously reported [35] under hydrothermal conditions at 150°C over 7 days from a solution of 1.0 FeO : 0.66 1,3,5-BTC : 2.0 HF : 1.2HNO₃ : 280 H₂O.

■ Encapsulation

Busulfan (99%, Fluka) encapsulation was performed by impregnation, choosing acetonitrile (99.9%, Aldrich) and dichloromethane (99.9%, Aldrich) as solvents according to the high solubility of busulfan in these solutions (30 and 10 mg/ml, respectively) and low boiling point necessary to facilitate the removal of residual solvent encapsulation. Busulfan solubility in these solvents was determined by dissolving overnight busulfan in excess in the solvents, separation of non dissolved crystals by ultracentrifugation, and assessment of busulfan concentration in the clear supernatants thus obtained.

For encapsulation studies, 25 mg of dried NPs of MIL-88A, MIL-89, MIL-100 (previously dehydrated at 100°C/16 h) and MIL-53 (previously dehydrated at 150°C/16 h) were suspended in 2.5 ml of freshly prepared busulfan solutions at 80% of the maximum solubility. The suspension was stirred for 16 h at room temperature. The busulfan-loaded NPs were then collected by centrifugation (5600 g) for 10 min and dried under vacuum at room temperature for 3 days. All experiments were performed in quadruplicate. Busulfan loadings were determined by elemental analysis and by NMR spectroscopy.

For the determination of the busulfan loading by NMR spectroscopy, 20 mg of MIL-100 and MIL-53 NPs (previously dried at 100°C and 150°C for 16 h, respectively) were incubated in 2 ml of a 10 mg/ml busulfan solution in heavy dichloromethane (CD₂Cl₂; Euriso-top, France), containing 1 μ l of acetonitrile, used as an internal standard. After 24 h of incubation at room temperature and under stirring, the NPs were recovered by centrifugation at 5600 g for 10 min and dried overnight under vacuum. The amount

of non encapsulated busulfan was determined in the supernatants by ¹H-NMR spectroscopy (300 MHz, Avance, Bruker), using a calibration curve of busulfan solutions in CD₂Cl₂ (0.1 to 10 g/l) containing 0.5 μ l/ml of acetonitrile. NMR(CD₂Cl₂) ¹H: 1.7 (4, CH₂, multiplet), 2.9 (6, CH₃, singlet), and 4.1 ppm (4, CH₂(SO₃); multiplet). Integrations of the peaks corresponding to busulfan (CH₃ singlet at 2.9 ppm) and acetonitrile (1.9 ppm) were used for the drug quantification.

Elemental analysis was performed on dried busulfan-loaded NPs, enabling determination of C, O and S wt%. This allowed a direct quantification of the amount of busulfan entrapped in the NPs.

Busulfan encapsulation efficiency was calculated as the percentage of drug effectively entrapped inside the NPs with regard to the total amount of drug used in the preparation procedure.

■ Busulfan release

The release of busulfan from the NPs of MIL-100 and MIL-53 was studied in a phosphate buffer solution (PBS) at pH 7.4, prepared using deuterated water (D₂O; Euriso-top, France). 25 mg of busulfan-containing NPs were suspended in 2 ml of PBS pH 7.4 at 37°C under continuous bidimensional stirring for different incubation times. After centrifugation at 5600 g for 10 min, aliquots of 1 ml each were periodically recovered and replaced with the same volume of fresh PBS. Released busulfan was quantified by ¹H-NMR using acetonitrile as internal standard, as explained before. NMR (PBS/D₂O) ¹H: 1.8 (4, CH₂, multiplet), 3.1 (6, CH₃, singlet), and 4.3 ppm (4, CH₂(SO₃), multiplet). The acetonitrile peak was at 2 ppm. Integrations of the peaks corresponding to busulfan (CH₃ singlet at 3.1 ppm) and acetonitrile (2 ppm) were used for the busulfan quantification.

■ *In vitro* cytotoxicity studies

The cytotoxicity of free busulfan, busulfan containing NPs of MIL-100 and empty MIL-100 NPs was analyzed in the following cell lines: CCRF-CEM (human leukemia), J774 (human macrophages) and RPMI-8226 (human multiple myeloma).

All cell lines were maintained in RPMI-1640 medium (Lonza) supplemented with 10% heat-inactivated fetal calf serum, 105 U/L Penicillin G and 100 mg/L streptomycin in 7.5 cm² tissue culture flasks in a humidified atmosphere of 5% carbon dioxide at 37°C.

Cells were plated on 96-well flat-bottom microtiter plates. Seven busulfan concentrations (range 0.246 $\mu\text{g/ml}$ to 2460 $\mu\text{g/ml}$: 0.001 mM to 10 mM) were made by serial dilutions of busulfan dissolved in DMSO. 2 μl of each concentration of busulfan solutions were added to 200 μl of the complete cell culture medium.

In parallel, seven concentrations of empty MIL-100 NPs (range 0.5 $\mu\text{g/ml}$ - 5000 $\mu\text{g/ml}$) and seven concentrations of busulfan loaded NPs ([busulfan] from 0.246 $\mu\text{g/ml}$ to 2460 $\mu\text{g/ml}$; i.e., from 0.001 mM to 10 mM) were suspended in RPMI-1640 medium. 20 μl of these suspensions of empty and busulfan-loaded NPs were added to 200 μl of the complete cell culture medium and the cells were exposed to 2 μl of DMSO corresponding to the quantity used in busulfan solutions.

After 48 h of incubation the chemosensitivity was evaluated by thiazolyl blue tetrazolium bromide (3-(4,5-Dimethylthiazol-2-yl)-2,5-diphenyltetrazolium bromide or MTT reagent; 98%; Aldrich) in PBS using the concentration of 5 mg/ml. 25 μl of this MTT reagent was added to each well. Within the next 3 h, mitochondrial aldehyde dehydrogenase of viable cells reduced the yellow soluble MTT reagent to water-insoluble blue formazan crystals. The plates of CCRF-CEM, RPMI-8226 (not the J774 because they are adherent cells) were centrifuged (500 g) for 5 min and then the medium was evacuated. To dissolve formazan crystals, 200 μl of DMSO were then added to each well in the case of J774 and RPMI-8226, and 75 μl to each well in the case of CCRF-CEM.

The absorbance of the dissolved formazan blue dye was measured at 570 nm using an automated Multiscan Ascent 7000 microplate reader (Thermolab Electron Co.) to enable the calculations.

■ Molecular modeling

The structure of the hybrid porous framework MIL-53(Fe) in presence of busulfan was first built from the unit cell parameters extracted from *in situ* XRPD (Space group $n^{\circ}15$, C2/c, with $a = 19.428 \text{ \AA}$, $b = 10.3546 \text{ \AA}$, $c = 6.9108 \text{ \AA}$, $\beta = 108.567^{\circ}$). Please note that micrometric particles of MIL-53 were used in order to obtain a better crystallinity enabling us to index the corresponding busulfan-loaded MIL-53 pattern. We used the computational assisted structure determination previously employed for investigating the MIL-53 series with various guest molecules [36,37] including ibuprofen [38]. Several starting geometries for one busulfan molecule

per pore of MIL-53(Fe) were generated by chemical intuition and we further checked that the energy optimization of such models always resulted in the same geometry. A (1,1,2) simulation cell of the MIL-53(Fe) was considered in these calculations in order to accommodate the inclusion of the busulfan molecule within the pore. The geometry optimization maintaining the cell parameters of the framework fixed, was then performed using a periodic Density Functional Theory calculation (DFT) with the PW91 GGA density functional [39], and the double numerical basis set containing polarization functions on hydrogen atoms (DNP) [40] as implemented in the DMol3 code [101]. The PW91 functional has been successfully used to describe the interactions between ibuprofen and the MIL-53(Fe) solid [38]. The interaction energy between busulfan and the MIL-53(Fe) solid was further evaluated by the difference between the energy of the busulfan/MIL-53Fe adduct and the energy sum of the single constituents. A further step consisted of following the same approach to investigate the busulfan/modified MIL-53(Fe)-NH₂ system as a test case in order to emphasize the effect of the grafting ligands on the structural and energetic features of the confined drug molecules. As an exploratory approach, the cell parameters of the MIL-53(Fe)-NH₂ structure in presence of busulfan were assumed to be the same as for the non-modified form.

Results

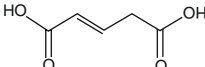
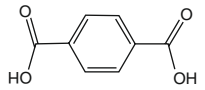
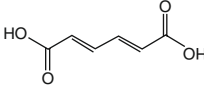
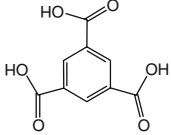
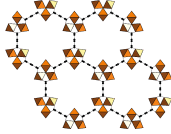
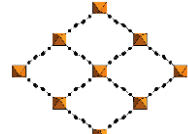
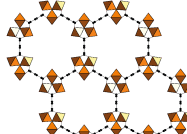
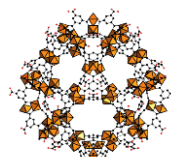
■ Synthesis of NPs

Nanoparticles of four types of crystalline porous iron(III) carboxylate solids, either with a flexible framework such as the iron fumarate MIL-88A, iron muconate MIL-89 or iron terephthalate MIL-53, or a rigid mesoporous iron trimesate MIL 100, were obtained (TABLE 1 & FIGURE 1) using various hydro- or solvo-thermal methods.

X-ray powder diffraction confirmed not only the crystal structure of the different hybrid NPs, but also the smaller particle size as indicated by the larger width of the Bragg peaks, as shown here for MIL-100 (FIGURE 2), compared with the MIL-100 microcrystals. A similar peak enlargement is also observed for MIL-88A, MIL-89 and MIL-53.

All NPs showed a faceted-type structure, as confirmed by SEM and TEM images (FIGURE 1). Nanoparticles of MIL-88A and MIL-89 exhibited the smallest sizes (~30–50 nm; FIGURE 1A & 1B). A rhombohedral shape with mean diameters around 100 nm were present for MIL-100

Table 1. Busulfan loading and structural features of several porous iron (III) carboxylate MOF nanoparticles.

	MIL-88A	MIL-53	MIL-89	MIL-100
Organic linker	Fumaric acid 	Terephthalic acid 	Muconic acid 	Trimesic acid 
Crystalline structure				
Flexibility	Yes	Yes	Yes	No
Pore size (Å)	6	8.5	11	25 (5.6) 29 (8.6)
Particle size (nm)	100 ± 25	350 ± 100*	75 ± 25	100 ± 50
Busulfan loadings (wt%) (elemental analysis)	8 ± 1	14 ± 2	10 ± 2	26 ± 3
Loading efficiency (%)	3 ± 1	18 ± 2	4 ± 1	32 ± 4
Busulfan loadings (wt %) (NMR)	–	13 ± 1	–	25 ± 1
Loading efficiency (%)	–	16 ± 1	–	30 ± 1

To encapsulate Busulfan, dichloromethane or acetonitrile were used as drug solvents in the case of MIL-53 and MIL-100, and MIL-88A and MIL-89, respectively. Drug loadings and entrapment efficiencies were assessed both by elemental analysis and NMR spectroscopy. All experiments were performed in triplicate.

NPs as observed by TEM (FIGURE 1D). In the case of MIL-53, particles possessed a bimodal distribution and contained besides NPs, some micrometric particles (1.2 ± 2 in length and $1.5 \pm 0.8 \mu\text{m}$ in width). This raises the difficulty of obtaining pure monodisperse NPs of MIL-53. The systematic study of the iron terephthalate based MOFs using solvothermal conditions has clearly shown previously that kinetically favored iron trimer MOFs are formed at shorter times or lower temperatures (MIL-88, MIL-101, MOF-235) while MIL-53, which is the thermodynamically favored product, is obtained at higher temperatures or using longer times. Indeed, the growth of MIL-53 is controlled by a dissolution-recrystallization process depending on the dissolution of the kinetic phase which would explain why larger micrometric rhombohedral crystals are obtained together with NPs of around 350 nm (FIGURE 1C). Comparatively, synthesis of MIL-53 in water led to rod-type NPs of about 6 μm length and 2.5 μm width (results not shown; [27]).

The NP size distributions determined by DLS are presented in TABLE 1. The sizes vary from 75 nm (MIL-89) up to approximately 350 nm (MIL-53). The polydispersities were comprised between 0.3 (MIL-88A and MIL-100) and more than 0.6 (MIL-53 and MIL-89), showing in the

latter cases the presence of several populations of NPs and/or aggregates, respectively.

■ Busulfan loading

Busulfan loading was determined using two complementary techniques: by direct dosage of busulfan in the NPs by elemental analysis and by indirect dosage of the nonentrapped busulfan in the supernatants recovered after centrifugations of the NPs suspensions by $^1\text{H-NMR}$.

Elemental analysis (TABLE 1) indicated a busulfan content of 8 and 10 wt% for MIL-88A and MIL-89 NPs, respectively, with low encapsulation efficiencies (3–4%), whereas MIL-53 and MIL-100 adsorbed higher contents, up to 14 and 26 wt%, respectively. The loading efficiencies reached 18 and 32 wt%, respectively.

NMR spectroscopy was then used to assess the loading into the best suited NPs (i.e., MIL-100 and MIL-53) (TABLE 1), in good agreement with the elemental analysis results. Busulfan loading into MIL-100 NPs was 25 wt% and 13 wt% in MIL-53. The encapsulation efficiencies were relatively high, 16 wt% (MIL-53) and 29 wt% (MIL-100).

XRPD of the busulfan containing MIL-100 (and MIL-53) NPs enabled confirmation of not only of the maintenance of its crystalline structure after drug encapsulation, but also the

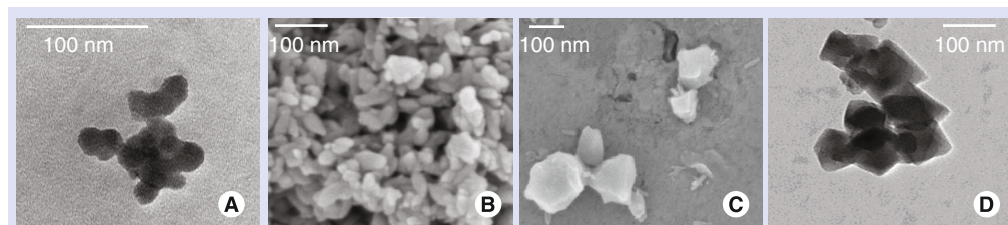


Figure 1. TEM and SEM pictures showing the morphology of various nanoparticles made of: (A) MIL-88A (TEM); (B) MIL-89 (SEM); (C) MIL-53 (SEM) and (D) MIL-100 (TEM).

absence of peaks issued from residual crystalline busulfan (FIGURE 2)

■ *In vitro* release

$^1\text{H-NMR}$ spectroscopy was used to follow busulfan release as it gave the most reproducible results among all other techniques tested, such as radioactivity counting using radiolabeled busulfan or dosage using elemental analysis. However, in the

NMR experiments it is not possible to use serum in the release media, as the peaks of the serum components strongly overlap with the busulfan peaks. In previous studies, we have performed comparative release studies in media containing or not containing serum in the case of other drugs, such as AZT showing that serum did not affect drug release [27].

Advantageously, $^1\text{H-NMR}$ spectroscopy was

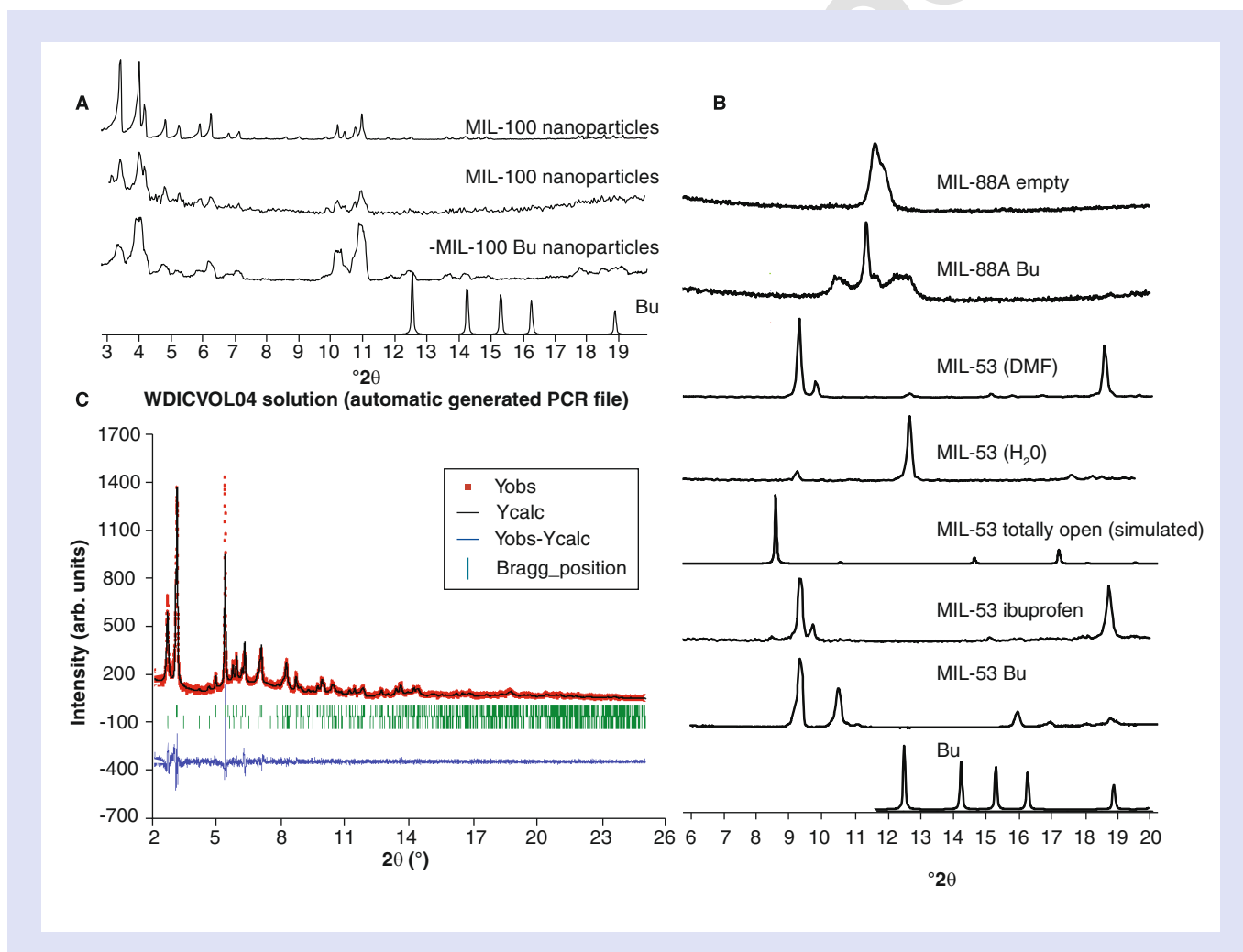


Figure 2. XRPD patterns ($\lambda\text{Cu}\sim 1.5406\text{\AA}$) of (A) MIL-100 micro and nanoparticles, busulfan containing MIL-100 nanoparticles and free crystalline busulfan; (B) Micrometric MIL-53 and MIL-88A with different pore contents: MIL-88A empty, busulfan-loaded MIL-88A, DMF-loaded MIL-53, hydrated MIL-53, large pores MIL-53, ibuprofen-loaded MIL-53, busulfan-loaded MIL-53 and free busulfan (from the top to the bottom) and (C) Pattern matching of the busulfan containing MIL-53 microparticles.

also used to study the integrity of the encapsulated drug. Indeed, busulfan readily degrades in water, [12,41], into tetrahydrofuran and methanesulphonic acid as shown by $^1\text{H-NMR}$ [12]. Noteworthy, the tetrahydrofuran resonance peaks ($(\text{CH}_2\text{-O}$, multiplet) and (CH_2) , multiplet)) and the methanesulphonic acid resonance peak (CH_3 , singlet) were not superimposed with the busulfan peaks [20]. These differences have been advantageously used previously to prove that busulfan conserved its integrity when encapsulated into biodegradable polymeric NPs [20]. In our case, in agreement with previously published data, [12,41] the busulfan NMR spectra in deuterated PBS showed three resonance peaks 1.8 (4, CH_2 , multiplet), 3.1 (6, CH_3 , singlet), and 4.3 ppm (4, $\text{CH}_2(\text{SO}_3)$, multiplet) (results not shown).

The $^1\text{H-NMR}$ spectra of busulfan released from MIL-100 and MIL-53 NPs (FIGURE 3) clearly show solely the presence of the characteristic peaks of busulfan (1.7, 2.9 and 4.1 ppm). The characteristic acetonitrile peak, used as internal standard, appeared at 2 ppm. No degradation products such as tetrahydrofuran and methanesulphonic acid could be detected, confirming the integrity of the released drug.

Additionally, the amount of busulfan released from the loaded NPs was quantified through the $^1\text{H-NMR}$ spectra of the supernatants obtained

after NP centrifugation (FIGURE 4). Two steps can be distinguished. First, within 30 min of incubation in PBS, 38 and 61% of the entrapped busulfan was released from the MIL-53 and MIL-100 NPs, respectively, while it reached 58% and 76% after 2 h, respectively. The second part of the release occurs in a slower manner.

■ Cytotoxicity tests

MTT assay for empty NPs

MTT toxicity assays were carried out on three different cells lines (human leukemia CCRF-CEM, human multiple myeloma RPMI-8226 and human macrophages J774) in contact with increasing concentrations of MIL-100 NPs. MTT data showed that these nanoMOFs were non toxic (cell viability >80%) up to concentrations of 50 $\mu\text{g/ml}$ (results not shown).

Activity tests

Similar tests were performed by incubating different concentrations of busulfan-containing MIL-100 NPs using the three cell lines mentioned above (CCRF-CEM, RPMI-8226 and J774). These NPs displayed similar cytotoxicity as free busulfan (FIGURE 5).

■ Molecular simulations

In order to analyze the successful entrapment of busulfan within the pores, from a practical

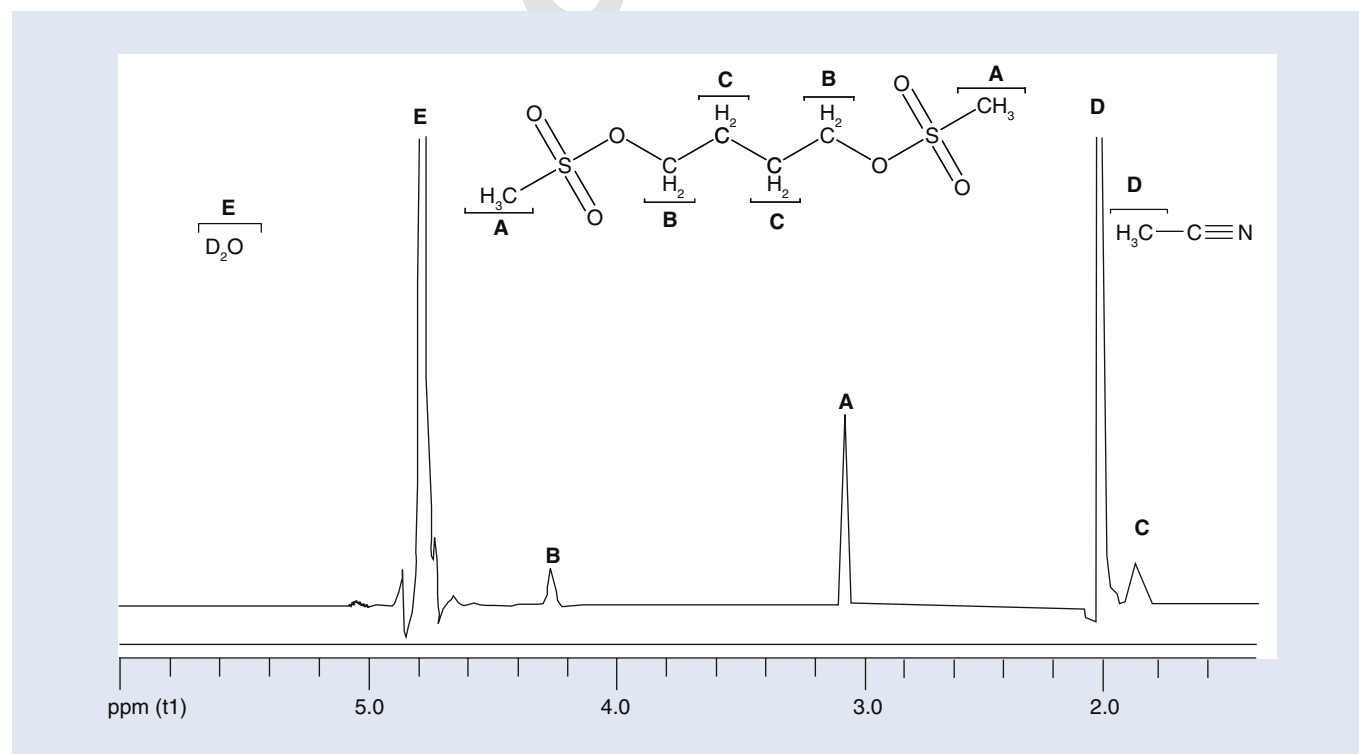


Figure 3. $^1\text{H-NMR}$ spectra (300 MHz) of released busulfan in PBS (D_2O) containing acetonitrile as an internal standard.

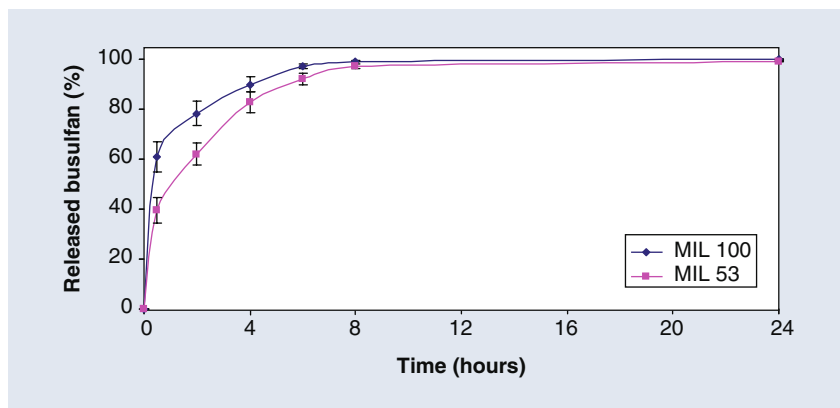


Figure 4. Busulfan release from MIL-100 and MIL-53 nanoparticles followed by $^1\text{H-NMR}$.

point of view, micrometric crystals instead of NPs of the flexible MIL-53 and MIL-88A solids were used in order to obtain a better crystallinity. XRPD patterns were thus compared with analogous solids with different pore contents leading to different cell volumes and symmetry, according to the size of the hosted molecule. Indeed, a high quality XRPD of busulfan containing MIL-53 solid, obtained right after busulfan encapsulation and drying, has been collected at room temperature and indexed using Dicvol. A mixture of two different pore opening phases was observed, one exhibiting a narrow pore form with a monoclinic cell (C2/c ($n^{\circ}15$) with $a = 19.428(1)$, $b = 10.3546(7)$, $c = 6.9108(4)$, $\beta = 108.567(5)$ Å; 1318 Å³) and one with a large pore form and an orthorhombic cell (Imcm $a = 16.490(1)$, $b = 13.653(1)$, $c = 6.8825(7)$ Å; 1549 Å³). Based on our previous experience related to the adsorption of guest species in flexible MOFs, this corresponds probably to the busulfan-MIL-53 form (narrow pores) and the busulfan/solvent MIL-53 form (large pores), respectively.

DFT calculations were performed on busulfan loaded MIL-53 in its narrow pores form, i.e., the one with the higher interaction energy between the busulfan and the framework. First, the optimized geometry reported in **FIGURE 6A** confirms that enough space is available with this narrow pores form to accommodate busulfan molecules within the porosity of the MIL-53(Fe). Second, busulfan is located in such a way to form strong hydrogen bonding between the oxygen of its sulfonate groups and the $\mu\text{-OH}$ hydroxyl group of the matrix, with characteristic O(sulfonate)-H($\mu\text{-OH}$) distances of 1.68 and 1.80 Å. In addition, weaker van der Waals and/or CH- π interactions are found between both sulfonate and methyl

groups of the busulfan molecule and the organic linker of MIL-53(Fe) represented in pink and white respectively. The so-obtained geometry leads to high drug-matrix interaction energy of $-69.6 \text{ kJ}\cdot\text{mol}^{-1}$.

Discussion

In spite of the recent intense interest in the field of nanometric MOFs, there are still scarce examples in the literature of such nanomaterials: gadolinium [42,43] or manganese carboxylates [44], mesoporous chromium terephthalate (MIL-101) [45] microporous zinc imidazolate (ZIF-8) [46] or carboxylates (MOF-5) [47,48] microporous copper trimesate [49] as well as iron carboxylates [27,46,50]. In most cases, highly toxic metals (Gd, Cr) were used and/or the NPs were obtained using toxic organic solvents [25,26]. Our approach uses simple synthesis methods, hydro/solvothermal or microwave assisted, of NPs of various porous hybrid non toxic iron carboxylates, with mean diameters of 75 up to around 350 nm (**TABLE 1**, **FIGURE 1** & **FIGURE 2**) [27].

Important amounts of busulfan (>8 wt%) could be loaded in all types of nanoMOFs. In the case of flexible MOFs (MIL-88A, MIL-89, MIL-53), loadings from 8 to 14 wt% represent real progress, as compared with the best loading reported so far being around 6 wt% [19,20,21,22]. However, a tremendous achievement was obtained through the loading of busulfan in MIL-100 NPs which reached 25 wt%, gaining a factor four in terms of entrapment. Such high encapsulation capacities are important, because the quantity of the carrier material needed to be administered to reach a given dose of drug may be reduced accordingly. Such an approach represents a clear improvement for the patients comfort as well as a competitive advantage from an industrial point of view.

The high loading obtained in the case of MIL-100 is undoubtedly attributed to its large pore volume ($V_p = 1.6 \text{ cm}^3\cdot\text{g}^{-1}$) compared with the other tested materials [27]. The absence of busulfan crystals in the MOF formulations (**FIGURE 2**), represents a main benefit since, in previous studies, busulfan-loaded NPs prepared by nanoprecipitation [20] showed the formation of numerous busulfan crystals in the NPs suspensions. This was clearly shown to be related to the high tendency of busulfan to crystallize in aqueous media [23,24] and during the NPs preparation process [19,20,21].

In the present study, busulfan was impregnated into the pores by a simple suspension of

the hybrid NPs in a busulfan solution, followed by the recovery of the NPs by centrifugation and drying. Therefore, busulfan crystallization was avoided since:

- The solubilization media of busulfan is the same during the whole entrapment procedure which was not the case with the nanoprecipitation procedure;

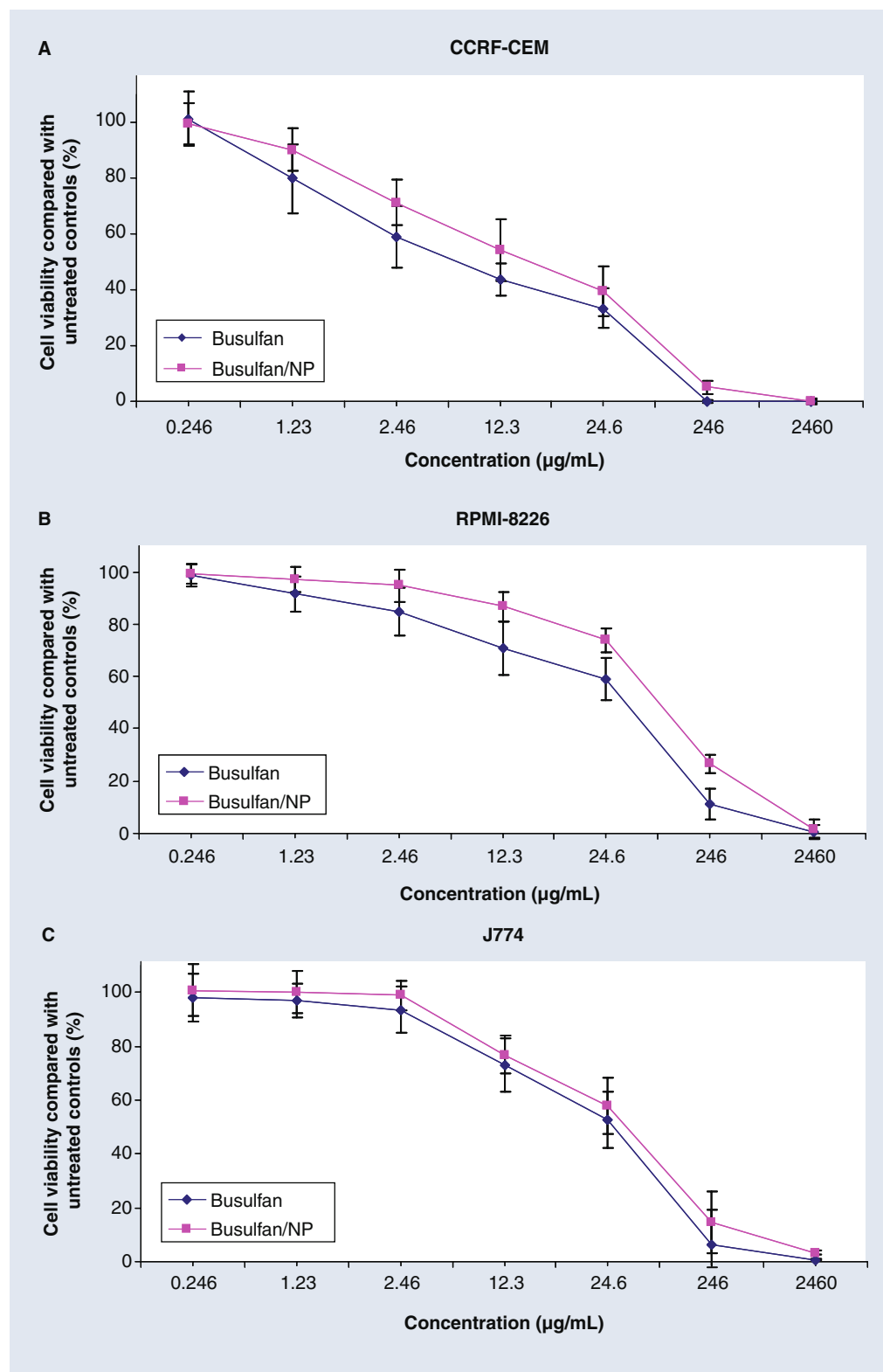


Figure 5. *In vitro* activity of free busulfan and busulfan-loaded in MIL-100 nanoparticles on: (A) CCRF-CEM, (B) RPMI-8226 and (C) J774 cells.

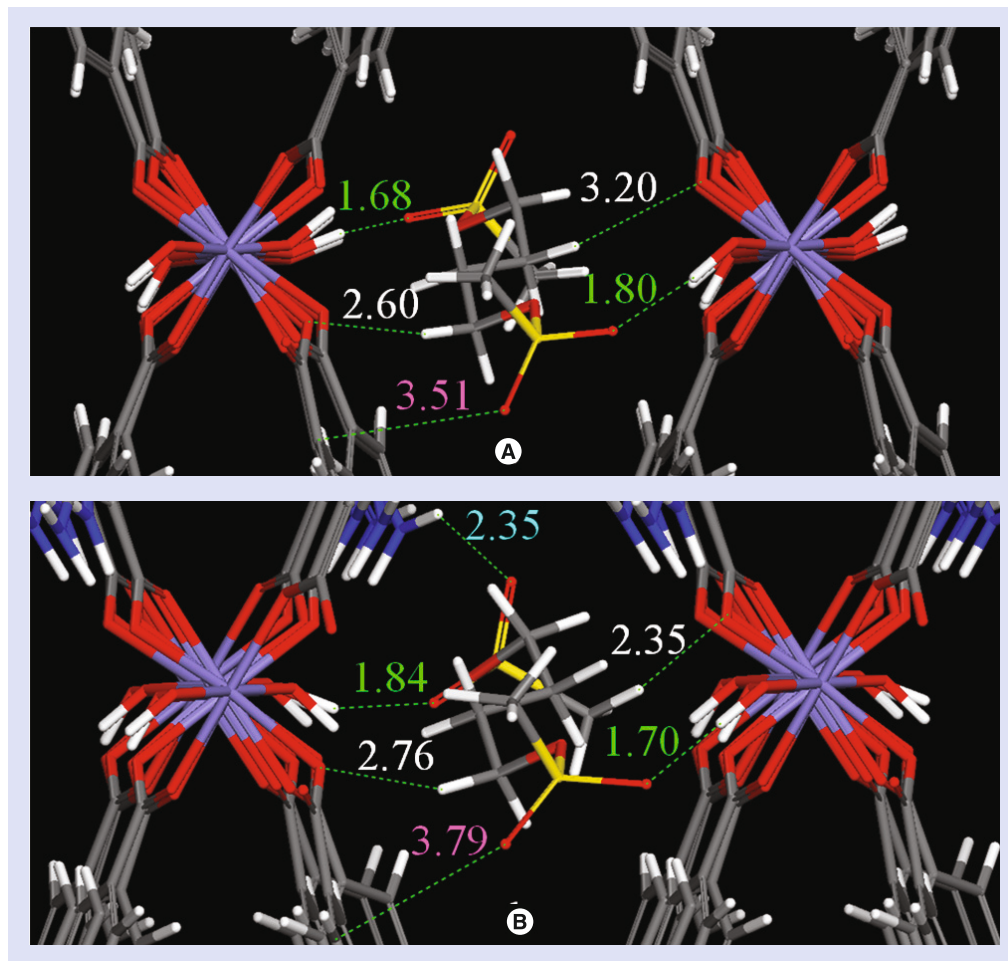


Figure 6 . DFT optimized geometries of the busulfan within the pores of the non modified MIL-53(Fe) (A) and of the functionalized MIL-53(Fe)-NH₂ (B). The different interactions between the busulfan and the host matrix are distinguished by colors and the distances are reported in Å.

- The concentrations of the starting busulfan solutions were chosen at only 80% of the drug maximum solubility in this solvent;
- Busulfan concentration in the medium decreased as busulfan was adsorbed into the pores of the NPs during the encapsulation process.

Considering the dimensions of the busulfan molecule (13.4×3.5 Å), compatible with the pore size of the selected MOFs, as well as the resulting important busulfan loading capacities, it is assumed that the drug is not only adsorbed onto the external surface of the NPs, but well encapsulated into their pores. Furthermore, it is well known that the flexible structure of porous MOFs can change upon the adsorption of guest molecules, such as busulfan. Molecular simulations assisted the investigation of the successful entrapment of busulfan within the MIL-53 pores. The optimized geometry (FIGURE 6A) showed that busulfan formed strong hydrogen

bonds with the matrix as well as weaker van der Waals and/or CH- π interactions. The resulting drug-matrix interaction energy of -69.6 kJ.mol⁻¹ is significantly higher than that previously observed for ibuprofen in the same host material (-57.4 kJ.mol⁻¹) [38]. Such a different energetic behavior is explained by the fact that the two sulfonate functions of busulfan interact strongly with the MIL-53(Fe) while for ibuprofen, only one carboxylate group was involved. Indeed, the obtained high binding energy shows that the presence of the μ 2-OH groups allows a strong linking of the busulfan molecules to the pore wall of the MIL-53(Fe) material, that can usually be attained in mesoporous materials only once their surfaces are functionalized [51].

NMR spectroscopy allowed checking busulfan release and integrity, with a full release of busulfan achieved in PBS in about 8 h (FIGURE 4). However, a large amount of busulfan was released in the first 30 min of incubation (61

and 38% in the case of MIL-100 and MIL-53 NPs). The higher degree of controlled release in the case of the MIL-53 is due either to the mono-dimensional smaller channels, the larger particle size of MIL-53 (TABLE 1), and/or the flexible character of MIL-53 slowing down the diffusion and increasing the drug-matrix interactions as shown by the DFT calculations.

One would expect that in the case of iron (III) carboxylate NPs, the amount of busulfan released within the first minutes of incubation could be further reduced by using appropriate linkers with a higher affinity for busulfan, bearing, for example amino groups. To that purpose, DFT calculations were performed for the busulfan/modified MIL-53(Fe)-NH₂, whereas the amino group was directly grafted on the aromatic ring of the terephthalate linker. As shown in FIGURE 6B, the preferential arrangement of the busulfan involves interactions between the oxygen atom of its sulfonate group and the NH₂ functional group grafted on the organic linker (represented in light blue arrows) with a characteristic distance of 2.45 Å, while those between the sulfonate groups and the μ2-OH hydroxyl group of the pore wall remain almost unchanged compared with the nonmodified MIL-53(Fe) form. The resulting interaction energy of -74.4 kJ.mol⁻¹ is almost 5 kJ.mol⁻¹ higher than in absence of functionalized linkers. The obtained geometry suggests that the presence of this amino group serves as additional anchoring points for the busulfan, as it was already observed for other drug molecules adsorbed in functionalized mesoporous materials [51]. Such an enhancement of the drug/matrix interactions that is expected to control the first step of the release, could lead to a more controlled drug delivery by significantly increasing the energy barrier required to be overpassed prior to triggering the delivery process.

Apart from the NMR studies, another proof of the integrity of the released busulfan was the preservation of its pharmacological activity (FIGURE 5). The activity data demonstrated that, in all cases, the NPs loaded with busulfan had a pharmacological activity comparable to the free drug in three cancer lines (CCRF-CEM and RPMI-8226).

Finally, the empty MIL-100 NPs were very well tolerated by the three studied macrophage and cancer cell lines (80% inhibitory concentration: IC80 >5000 μg/ml for J774 and RPMI-8226 cells, and IC80 ~1000 μg/ml for CCRF-CEM cells).

Moreover, the cytotoxicity of these nano-MOFs has been recently assessed by an electric bioimpedance method using two different human hepatocyte cell lines (HepG2 and Hep3B), showing the low toxicity of the nanosuspensions [HORCAJADA ET AL., UNPUBLISHED DATA]. The more sensible Hep3B line, however, showed slight cytotoxic effects after the contact with 10–50 μg of MIL-100(Fe)/ml. Studies are underway to evaluate the cytotoxicity of different porous iron carboxylate nanoMOF as a function of their structure and composition. Tests such as membrane rupture (LDH), metabolic activity, cell viability and mitochondrial activity, as well as hemolysis assays will be performed in the near future.

These toxicity data corroborate our previously reported good *in vivo* tolerance of the NPs, synthesized in water or in the presence of DMF [27,33]. Indeed, the low toxicity achieved using iron was expected, since this metal is usually present in the body at relatively high concentrations (4 g in an adult; DL50 = 30 g/kg) [52,102], unlike toxic metals (Cr, Cu, Co, Cd, Ni, Ln.) [53], typically used to prepare MOFs. In addition, the use of toxic solvents in the synthesis of these NPs was avoided as much as possible, by setting up procedures to synthesize the MOF NPs under hydrothermal conditions, and a special attention was paid to extensively wash the NPs to remove trace of solvents if present.

Studies are underway to coat the NPs' surface with PEG chains which have been shown to reduce liver accumulation [54,55].

Conclusion

MOF NPs with their wide range of composition, structure, tunable pore size, high pore volume and lack of toxicity make them very promising candidates for busulfan delivery. High drug payloads and absence of crystallisation were obtained, allowing the release of intact busulfan molecules. Further functionalization of the nanoMOFs surface with PEG should allow avoidance of liver accumulation which, in turn, should reduce busulfan toxicity and side effects.

Future perspective

There is a great interest in the development of nanocarriers for busulfan alkylating agent that are widely used in chemotherapy, but cause severe side effects. The promising loadings obtained using MOF NPs could be further improved by using tailor-made biocompatible coordination polymers, taking advantage of their tunable composition, structure, pore size and volume,

easy functionalization, flexible network and/or accessible metal sites. Moreover, further studies should focus on the design of 'stealth' NPs able to release busulfan in a controlled manner.

Acknowledgements

We acknowledge V. Agostoni and J.F. Eubank for their help with the experiments, D. Jaillard and N. Tsapis for TEM and SEM characterization. We are indebted to C. Robert-Labarre and Z. Chiekh Ali for the NMR studies, V. Marsaud for the MTT and activity studies and Y. Filinchuk at ESRF for the Synchrotron study.

Financial & competing interests disclosure

This work was partially supported by the CNRS, Université Paris Sud, Université de Versailles Saint-Quentin, Université Montpellier 2, Nanogalenic network and EU

funding through the ERC-2007–209241-BioMOFs and EU funding through the ITN 237962 Cyclon. The authors have no other relevant affiliations or financial involvement with any organization or entity with a financial interest in or financial conflict with the subject matter or materials discussed in the manuscript apart from those disclosed.

No writing assistance was utilized in the production of this manuscript.

Ethical conduct of research

The authors state that they have obtained appropriate institutional review board approval or have followed the principles outlined in the Declaration of Helsinki for all human or animal experimental investigations. In addition, for investigations involving human subjects, informed consent has been obtained from the participants involved.

Executive summary

- Busulfan is an amphiphilic molecule with a strong tendency to crystallize and to degrade in aqueous solutions, making its entrapment in conventional polymeric drug carriers a challenge.
- Busulfan could be efficiently entrapped in hybrid crystalline nanoMOF (loadings up to 25 wt%)
- NanoMOF formulations have kept busulfan in molecular form, preventing its crystallization and degradation
- Released busulfan was intact and maintained its pharmacological activity

Bibliography

Papers of special note have been highlighted as:

▪ of interest

▪▪ of considerable interest

- 1 Dunn CDR. The chemical and biological properties of busulfan ('Myleran'). *Hemat.* 2, 101–117 (1974).
- 2 Galton DAG. Myleran in chronic myeloid leukemia: results of treatment. *Lancet* 1, 208–213 (1953).
- 3 Blazar BR, Ramsay NKC, Kersey JH, Krivik W, Arthur DC, Filipovich AH. Pretransplant conditioning with busulfan (Myleran) and cyclophosphamide for nonmalignant diseases. *Transplantation* 39(6), 597–603 (1985).
- 4 Hartmann O, Benhamou E, Beaujean F *et al.* High-dose busulfan and cyclophosphamide with autologous bone marrow transplantation support in advanced malignancies in children: a Phase II study. *J. Clin. Oncol.* 4, 1804–1810 (1986).
- 5 Santos GW. The Development of Busulfan/Cyclophosphamide Preparative Regimens. *Seminars in Oncology*. 20, 12–16 (1993).
- 6 Hassan M, Oberg G, Bekassy AN *et al.* Pharmacokinetics of high-dose busulfan in relation to age and chronopharmacology. *Cancer Chemother. Pharmacol.* 28(2) 130–134 (1991).
- 7 Meresse V, Hartmann O, Vassal G *et al.* Risk factors for hepatic veno-occlusive disease after high-dose busulfan-containing regimens followed by autologous bone marrow transplantation: a study in 136 children. *Bone Marrow Transplant.* 10, 135–141 (1992).
- 8 McDonald GB, Hinds MS, Fisher LD *et al.* Veno-occlusive disease of the liver and multiorgan failure after bone marrow transplantation: a cohort study of 355 patients. *Ann. Intern. Med.* 118, 255–267 (1993).
- 9 Grochow LB, Jones RJ, Brundrett RB *et al.* Pharmacokinetics of busulfan: correlation with veno-occlusive disease in patients undergoing bone marrow transplantation. *Cancer Chemother. Pharmacol.* 25(1), 55–61 (1989).
- 10 Bouligand J, Boland I, Valteau-Couanet D *et al.* In children and adolescents, the pharmacodynamics of high-dose busulfan is dependent on the second alkylating agent used in the combined regimen (melphalan or thiotepa). *Bone Marrow Transplant.* 32, 979–986 (2003).
- 11 Hassan M, Ehrsson H, Ljungman P. Aspects concerning busulfan pharmacokinetics and bioavailability. *Leuk. Lymphoma* 22, 395–407 (1996).
- 12 Hassan M, Ehrsson H. Degradation of busulfan in aqueous solution. *J. Pharm. Biomed. Anal.* 4, 95–101 (1986).
- **Results showing the fast degradation of Busulfan in aqueous media, a main drawback of this drug**
- 13 Bhagwatwar HP, Phadungpojina S, Chow DS, Andersson BS. Formulation and stability of busulfan for intravenous administration in high-dose chemotherapy. *Cancer Chemother. Pharmacol.* 37, 401–408 (1996).
- 14 Schuler US, Ehrsam M, Schneider A, Schmidt H, Deeg J, Ehninger G. Pharmacokinetics of intravenous busulfan and evaluation of the bioavailability of the oral formulation in conditioning for haematopoietic stem cell transplantation. *Bone Marrow Transplant.* 22, 241–244 (1998).
- 15 Andersson BS, Kashyap A, Couriel D *et al.* Intravenous busulfan in pretransplant chemotherapy: bioavailability and patient benefit. *Biol. Blood Marrow Transplant.* 9, 722–724 (2003).
- 16 Nguyen L, Fuller D, Lennon S, Leger F, Puozzo C. I.V. busulfan in pediatrics: a novel dosing to improve safety/efficacy for hematopoietic progenitor cell transplantation recipients. *Bone Marrow Transplant.* 33, 979–987 (2004).
- 17 Hassan Z, Nilsson C, Hassan M. Liposomal busulfan: bioavailability and effect on bone marrow in mice. *Bone Marrow Transplant.* 22, 913–918 (1998).
- 18 Olavarria E, Hassan M, Eades A *et al.* A Phase I/II study of multiple-dose intravenous busulfan as myeloablation prior to stem cell transplantation. *Leukemia* 14, 1954–1959 (2000).
- 19 Layre AM, Gref R, Richard J *et al.*

- Nanoencapsulation of a crystalline drug. *Int. J. Pharm.* 298(2), 323–327 (2005).
- 20 Layre A, Couvreur P, Chacun H *et al.* Busulfan loading into poly (alkyl cyanoacrylate) nanoparticles: Physico-chemistry and molecular modelling. *J. Biomed. Mater. Res. B Appl. Biomater.* 79(2), 254–262 (2006).
- 21 Layre A, Couvreur P, Chacun H *et al.* Novel composite core-shell nanoparticles as busulfan carriers. *J. Contr. Release* 111(3), 271–280 (2006).
- **Presents a strategy to entrap busulfan in biodegradable polymeric nanoparticles, achieving the highest drug payloads with polyalkylcyanoacrylates**
- 22 Layre A, Couvreur P, Richard J, Requier D, Ghermani N, Gref R. Freeze-drying of composite core-shell nanoparticles. *Drug Dev. Ind. Pharm.* 32(7), 839–846 (2006).
- 23 Bouligand J, Couvreur P, Layre AM *et al.* Busulphan-loaded long-circulating nanospheres, a very attractive challenge for both galenists and pharmacologists. *J. Microencapsul.* 24, 715–730 (2007).
- **Based on a physicochemical approach, the paper highlights the challenges related to busulfan entrapment in nanocarriers**
- 24 Ghermani NE, Spasojevic-de Bire A, Bouhmaida N *et al.* Molecular reactivity of busulfan through its experimental electrostatic properties in the solid state. *Pharm. Res.* 21, 598–607 (2004).
- 25 Férey G. Hybrid porous solids: past, present, future. *Chem. Soc. Rev.* 37, 191–241 (2008).
- 26 Férey G, Serre C. Large breathing effects in three-dimensional porous hybrid matter: facts, analyses, rules and consequences. *Chem. Soc. Rev.* 38, 1380–1399 (2009).
- 27 Horcajada P, Chalati T, Serre C *et al.* Porous metal-organic-framework nanocarriers as a potential platform for drug delivery and imaging. *Nat. Mater.* 9, 172–178 (2010).
- **First paper dealing with busulfan entrapment inside porous iron carboxylate MOF nanoparticles**
- 28 Whitfield TR, Wang X, Liu L, Jacobson AJ. Metal-organic frameworks based on iron oxide octahedral chains connected by benzenedicarboxylate dianions. *Solid State Sci.* 7, 1096–1103 (2005).
- 29 Horcajada P, Surlé S, Serre C *et al.* Synthesis and catalytic properties of MIL-100(Fe), an iron(III) carboxylate with large pores. *Chem. Commun.* 27, 2820–2822 (2007).
- **Paper presenting the synthesis and structure of iron trimesate MOF**
- 30 Serre C, Mellot-Draznieks C, Surlé S, Audebrand N, Filinchuk Y, Férey G. Role of solvent-host interactions that lead to very large swelling of hybrid frameworks. *Science* 315, 1828–1831 (2007).
- 31 Serre C, Millange F, Surlé S, Férey G. A route to the synthesis of trivalent transition-metal porous carboxylates with trimeric secondary building units. *Angew. Chem. Int. Ed.* 43, 6285–6289 (2004).
- 32 Surlé S, Serre C, Mellot-Draznieks C, Millange F, Férey G. A new isorectical class of metal organic-frameworks with the MIL-88 topology. *Chem. Commun.* 3, 284–286 (2006).
- 33 Chalati T, Horcajada P, Gref R, Couvreur P, Serre C. Optimisation of the synthesis of MOF nanoparticles made of flexible porous iron fumarate MIL-88A. *J. Mater. Chem.* 21, 2220–2227 (2011).
- 34 Dziobkowski CT, Wroblewski JT, Brown DB. Magnetic properties and Moessbauer spectra of several iron(III)-dicarboxylic acid complexes. *Inorg. Chem.* 20(3), 671–678 (1981).
- 35 Horcajada P, Surlé S, Serre C *et al.* Synthesis and catalytic properties of MIL-100(Fe), an iron(III) carboxylate with large pores. *Chem. Commun.* 2820–2822 (2007).
- 36 Llewellyn PL, Horcajada P, Maurin G *et al.* Complex adsorption of short linear alkanes in the flexible metal-organic-framework MIL-53(Fe). *J. Am. Chem. Soc.* 131, 13002–13008 (2009).
- 37 Devic T, Horcajada P, Serre C *et al.* Functionalization in flexible porous solids: effects on the pore opening and the host-guest interactions. *J. Am. Chem. Soc.* 132(3), 1127–1136 (2010).
- 38 Horcajada P, Serre C, Maurin G *et al.* Flexible porous metal-organic frameworks for a controlled drug delivery. *J. Am. Chem. Soc.* 130, 6774–6780 (2008).
- 39 Perdew JP, Wang Y. Accurate and simple analytic representation of the electron-gas correlation energy. *Phys. Rev. B* 45, 13244–13249 (1992).
- 40 Hehre WJ, Ditchfield R, Pople JA. Self-consistent molecular orbital methods. XII. Further extensions of Gaussian type basis sets for use in molecular orbital studies of organic molecules. *J. Chem. Phys.* 56, 2257–2261 (1972).
- 41 Feit PW, Rastrup-Andersen N. 4-Methanesulfonyloxybutanol: hydrolysis of busulfan. *J. Pharm. Sci.* 62, 1007–1008 (1973).
- 42 Rieter WJ, Taylor KML, An H, Lin W. Nanoscale metal-organic frameworks as potential multimodal contrast enhancing agents. *J. Am. Chem. Soc.* 128, 9024–9025 (2006).
- 43 Taylor KML, Jin A, Lin W. Surfactant-assisted synthesis of nanoscale gadolinium metal-organic frameworks for potential multimodal imaging. *Angew. Chem. Int. Ed.* 47, 7722–7725 (2008).
- 44 Taylor KML, Rieter WJ, Lin W. Manganese-based nanoscale metal-organic frameworks for magnetic resonance imaging. *J. Am. Chem. Soc.* 130, 14358–14359 (2008).
- 45 Demessence A, Horcajada P, Serre C *et al.* Elaboration and properties of hierarchically structured optical thin films of MIL-101(Cr). *Chem. Commun.* 14(46), 7149–7151 (2009).
- 46 Cravillon J, Munzer S, Lohmeier SJ, Feldhoff A, Huber K, Wiebcke M. Rapid room-temperature synthesis and characterization of nanocrystals of a prototypical zeolitic imidazolate framework. *Chem. Mater.* 21(8), 1410–1412 (2009).
- 47 Hermes S, Witte T, Hikov T *et al.* Trapping metal-organic framework nanocrystals: an in-situ time-resolved light scattering study on the crystal growth of MOF-5 in solution. *J. Am. Chem. Soc.* 129(17), 5324–5325 (2007).
- 48 Qiu LG, Li ZQ, Wu Y, Wang W, Xu T, Jiang X. Facile synthesis of nanocrystals of a microporous metal-organic framework by an ultrasonic method and selective sensing of organoamines. *Chem. Comm.* 31, 3642–3644 (2008).
- 49 Li ZQ, Qiu LG, Su T *et al.* Ultrasonic synthesis of the microporous metal-organic framework Cu₃(BTC)₂ at ambient temperature and pressure: an efficient and environmentally friendly method. *Mater. Lett.* 63(1), 78–80 (2009).
- 50 Horcajada P, Serre C, Grosso D *et al.* Colloidal route for preparing optical thin films of nanoporous metal-organic frameworks. *Adv. Mater.* 21, 1931–1935 (2009).
- 51 Vallet-Reghi M, Colilla M, Gonzalez B. Medical applications of organic-inorganic hybrid materials within the field of silica-based bioceramics. *Chem. Soc. Rev.* 40, 596–607 (2011).
- 52 Sheftel VO. *Indirect food additives and polymers: migration and toxicology.* Ministry of Health, (Lewis Publishers Inc.) Jerusalem, Israel, 148–154 (2000).
- 53 Goyer RA. Toxic effects of metals. in: casarett & doull's toxicology. The Basic Science of Poisons. Klaassen CD (Ed). McGraw-Hill Health professions division, NY, USA, (1996).
- 54 Klibanov AL, Maruyama K, Torchilin VP, Huang L. Amphiphatic polyethyleneglycols effectively prolong the circulation time of liposomes. *FEBS Lett.* 268, 235–237 (1990).
- 55 Gref R, Minamitake Y, Peracchia MT,

Trubetskoy V, Torchilin V, Langer R.
Biodegradable long circulating polymeric
nanospheres. *Science* 263, 1600–1603 (1994).

- First paper dealing with PEG surface
modification of biodegradable nanoparticles.

■ Websites

101 Accelrys DMol3Code: DMol3, v.4.0,
Accelrys, Inc.: San Diego, CA, USA (2005).

102 [www.chem.unep.ch/irptc/sids/
OECD/SIDS/100-121-120.pdf](http://www.chem.unep.ch/irptc/sids/OECD/SIDS/100-121-120.pdf) (2008).

Author Proof